Inorganic Chemistry

ARTICLE

pubs.acs.org/IC

Eu^{3+}:Y_2O_3 Microspheres and Microcubes: A Supercritical Synthesis and Characterization

M Kempaiah Devaraju,* Shu Yin, and Tsugio Sato

Institute of Multidisciplinary Research for Advanced Materials, Tohoku University, 2-1-1, Katahira, Aoba-ku, Sendai 980-8577, Japan

Supporting Information

ABSTRACT: A new approach that uses mixed supercritical solvents of water/1-propanol and water/methanol (400 °C, 40 MPa) to prepare morphology-controlled precursor materials in a very short reaction time, such as 10 min, followed by calcinations has been developed to form Eu^{3+}:Y_2O_3 microspheres of 2−3 μm in diameter or microcubes of 2−3 μm in side length, respectively. Eu^{3+}:Y_2O_3 microspheres and microcubes exhibited strong red emission at 610 nm corresponding to $^5D_0 \rightarrow {}^7F_2$ transition. The highest photoluminescence emission was obtained for the microspheres after calcination at 1000 °C for 1 h in air.

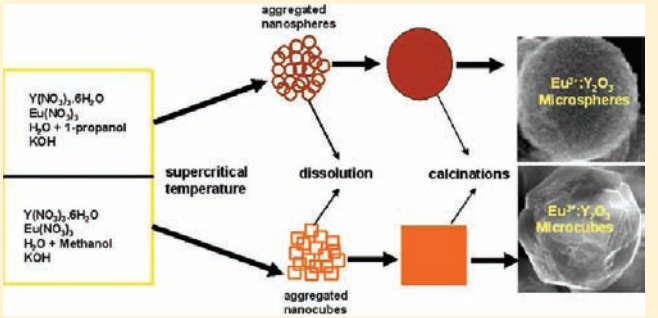

INTRODUCTION

In recent years, rare earth compounds have been widely used as high-performance luminescent devices, magnets, catalysts, and other functional materials based on their unique electronic, optical, and chemical characteristics arising from the 4f electrons.[1] Moreover, rare earth phosphors are technologically important materials for display applications, and the most important properties for such applications are high luminance intensity and long lifetime. Activated oxide phosphors doped with rare earth elements are investigated extensively in order to enhance the luminescence. Europium-doped yttria (Eu^{3+}:Y_2O_3) is an efficient red-emission phosphor and has been used in fluorescent lights (FL) and cathode ray tubes (CRT).[2] Recent studies show that Eu^{3+}:Y_2O_3 nanoparticles have significant promise in field emission displays (FED) and plasma display panels (PDP).[3,4] The ideal morphology of phosphor particles includes a perfect spherical shape, narrow size distribution, and nonagglomeration. Spherical morphology of the phosphors is good for high brightness and high resolution because of the high packing densities and low scattering of light.[5−11] The development of nano- or micromaterials with size- and shape-controlled morphologies may open new opportunities in exploring the chemical and physical properties of the materials.[12] Therefore, the design and controlled synthesis of inorganic materials with desired sizes and shapes has drawn considerable attention for many years.[13−18]

Over the last decade, many methods for the synthesis of rare earth oxide doped Y_2O_3 phosphors have been reported, including the solution combustion method,[19] the sol−gel method,[20] the spray pyrolysis method,[21] hydrothermal synthesis,[22] the precipitation method,[23] and the solvothermal refluxing method.[24,25] Recently, we reported the synthesis of Tb^{3+}-doped Y_2O_3 hollow microspheres by a supercritical solvothermal reaction followed by calcinations.[26] Supercritical reactions have recently been used for the synthesis of variety of inorganic materials.[27,28]

Herein, we present a simple and quick synthesis of Eu^{3+}:Y_2O_3 microspheres or microcubes via solvothermal supercritical reaction followed by calcinations, in which the precursors were prepared in 10 min of reaction time using mixed solutions such as water/1-propanol and water/methanol as reacting solvents. The supercritical solvothermal method provides a rapid crystallization, phase purity, and high yield.

EXPERIMENTAL SECTION

Reagents. Analytical grade $Y(NO_3)_3 \cdot 6H_2O$ and Eu_2O_3 (99.99%) were purchased from Kanto Chemical Co., Inc., Japan, and used without further purification. $Eu(NO_3)_3$ aqueous solution was obtained by dissolving Eu_2O_3 (99.99%) in diluted HNO_3 solution.

Synthesis of Eu^{3+}:Y_2O_3 Microspheres and Microcubes. In a typical synthesis procedure, 20 mL of 0.95 mmol of $Y(NO_3)_3 \cdot 6H_2O$ and 0.05 mmol of $Eu(NO_3)_3$ mixed aqueous solution and 15 mL of 1-propanol or methanol were taken in a separate beakers with vigorous stirring for 10 min, and the solution pH was adjusted to 7 using 5 mL of diluted KOH solution, that is, water/organic solvents volume ratio was 25/15. Finally, 10 mL of resulting mixture was transferred into a batch reactor of internal volume of 20 mL and heated at 400 °C for 10 min. The products were washed with distilled water and ethanol three times each and dried in air at 60 °C. The final products were obtained through a heat treatment at desired temperatures in air for 1 h with a heating rate of 2 °C min^{-1}.

The reference sample was prepared via a conventional coprecipitation calcination method, and similar grade source materials were used for the preparation of the reference sample. In a typical preparation, 100 mL of

Received: July 26, 2010
Published: May 06, 2011

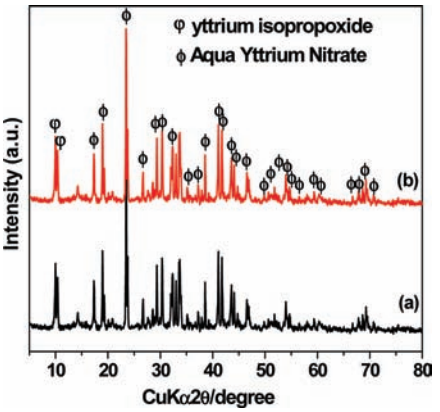

Figure 1. XRD patterns of as-synthesized products in mixed solvents of (a) water/1-propanol and (b) water/methanol at 400 °C for 10 min.

0.95 mmol of $Y(NO_3)_3 \cdot 6H_2O$ and 0.05 mmol of $Eu(NO_3)_3$ mixed aqueous solution was taken in a beaker and stirred for 15 min, and then dilute ammonia was added to precipitate the product. The precipitate was centrifuged, washed with water and ethanol, and dried. The dried product was calcined at 1000 °C for 1 h in air to obtain the desired 5 mol % doped Y_2O_3 powder.

Characterization. The crystal structure of the sample was determined by X-ray diffraction analysis (XRD, Shimadzu XD-D1) using graphite-monochromized Cu Kα radiation. The calcination temperature of the sample was determined by thermogravimetry−differential thermal analysis (TG−DTA, Rigaku TAS-200). The field emission scanning electron microscopy (FESEM) images were obtained with a Hitachi S4800 operated at beam energy of 15.0 kV. The morphology and size of the samples were determined by a transmission electron micrograph obtained on TEM, JEOL JEM-2010 with an accelerating voltage of 200 kV. EDS spectra were obtained on Hitachi S4800 with an accelerating voltage of 20 kV. The photoluminescence spectra were measured by a spectrofluorophotometer using 450 W xenon lamp (Shimadzu RF-5300P) at room temperature and a xenon−mercury pulse lamp for lifetime measurements.

RESULTS AND DISCUSSION

Crystalline Phase and Chemical Composition Analysis. Figure 1a,b shows the XRD patterns of as-synthesized product using mixed solvents of (a) water/1-propanol and (b) water/methanol at 400 °C and ca. 40 MPa. The crystalline phase of the as-synthesized products was identified as mixed phases of yttrium aqua nitrate $\{[Y(H_2O)_5(NO_3)_2(Y(H_2O)_2(NO_3)_4)\}$ (JCPDS card 84-0079) and yttrium isopropoxide ($YO_3C_9H_{21}$) (JCPDS card 19-1794). All the diffraction peaks could be well indexed to those phases.

FTIR spectra have been recorded for as-synthesized products to confirm the presence of nitrate and hydroxyl group. Figure 2a, b shows the FTIR spectra of as-synthesized product in mixed solvents of (a) water/1-propanol and (b) water/methanol. The absorption band corresponding to NO_3 appeared around 1353[29] and 819 cm^{-1}[130] in both the as-synthesized products. The stretching modes of OH around 3653 cm^{-1}, H_2O around 1630 cm^{-1}, and Y−O around 558 cm^{-1}[131] were also noticed in the IR spectra. These IR spectra data accorded with the XRD data shown in Figure 1. The calcined products exhibited a stretching mode of Y−O around 558 cm^{-1}. The peaks around 1400−1507 cm^{-1} might be attributed to CO_3 from air atmosphere.

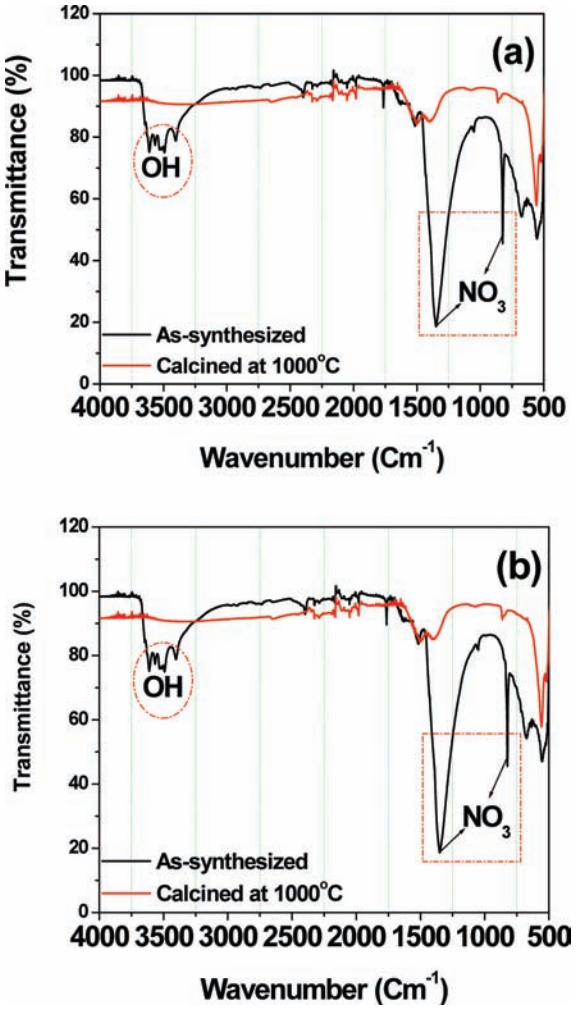

Figure 2. FTIR spectra of as-synthesized products in mixed solvents of (a) water/1-propanol and (b) water/methanol at 400 °C for 10 min.

Further, TG−DTA analysis was undertaken to support the XRD and IR data. Figure 3a,b shows the TG−DTA curves of as-synthesized product at 400 °C using mixed solvents of (a) water/1-propanol and (b) water/methanol, respectively. Both samples showed two-step weight losses until 1000 °C, and then the weight was almost constant. The first weight loss of 6.5% and 6.83% at 150−630 °C associated with four exothermic peaks might be due to elimination of adsorbed water and organics adsorbed on the surface of the products. The second weight losses of 77.43% and 77.13% at 630−995 °C might be due to the removal of residual structural water and denitrification. The second weight loss is much closer to the calculated value of 76% according to the reactions expressed by eqs 1 and 2, indicating that the samples contained a large amount of water and organic molecules adsorbed on the surface. However, both as-synthesized products exhibited quite a large amount of total weight loss, 83.94% and 83.96%, respectively.

$$[Y(H_2O)_5(NO_3)_2Y(H_2O)(NO_3)_4] \rightarrow Y_2O_3 + 6NO_2 + O_2 + 6H_2O \quad (1)$$

$$2YO_3C_9H_{21} \rightarrow Y_2O_3 + C_{18}H_{36} + 3H_2O \quad (2)$$

dx.doi.org/10.1021/ic101496b |Inorg. Chem. 2011, 50, 4698–4704

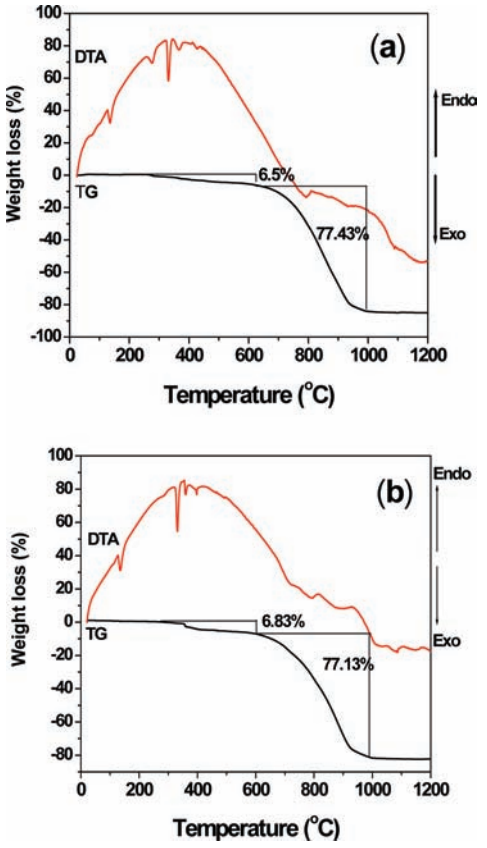

Figure 3. TG−DTA curves of as-synthesized products in mixed solvents of (a) water/1-propanol and (b) water/methanol at 400 °C for 10 min.

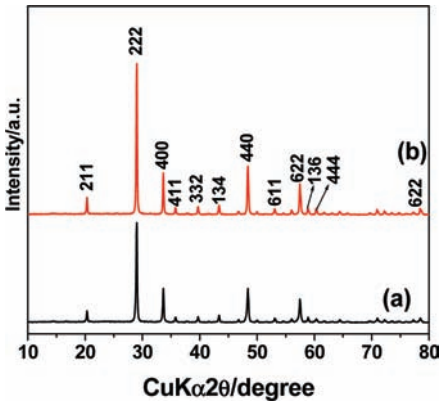

Figure 4. XRD patterns of Eu^{3+}:Y_2O_3 microspheres and microcubes after calcining the as-synthesized products in mixed solvents of (a) water/1-propanol and (b) water/methanol at 1000 °C for 1 h.

A similar large amount of weight loss was also observed in our previous study, which used organic solvents.[26]

Figure 4a,b shows the XRD patterns of the products calcined at 1000 °C for 1 h in air after the reactions in the mixed solvents of (a) water/1-propanol and (b) water/methanol at 400 °C for 10 min. All the diffraction peaks could be assigned to cubic Y_2O_3 (JCPDS file 70-0603) as shown in the figure. The particle size was calculated from Scherer's equation, $D = 0.89\lambda/(\beta \cos \theta)$, where D is the average crystallite size, λ is the X-ray wavelength (0.154 05 nm), and β is the full width at half-maximum intensity

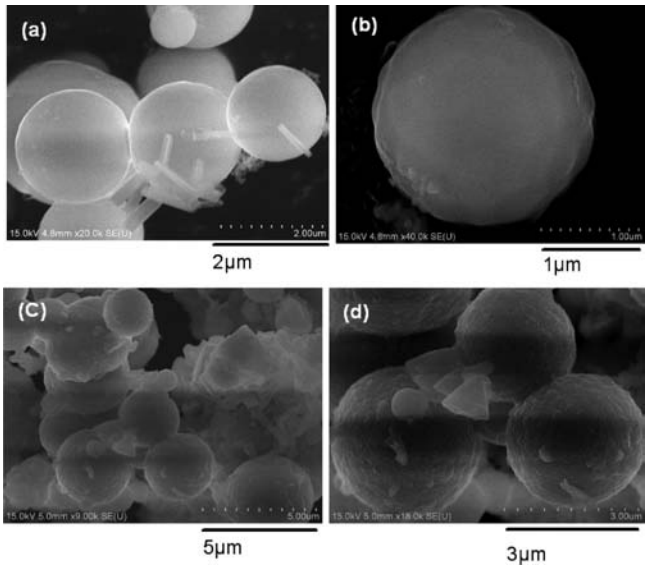

Figure 5. FESEM images of as-synthesized microspheres in water/1-propanol mixed solvent at 400 °C for 10 min (a, b) and Eu^{3+}:Y_2O_3 microspheres (c, d) prepared by calcination at 1000 °C for 1 h in air.

and diffraction angle θ of an observed peak, respectively. The strongest peak at $2\theta = 29.1°$ was used to calculate the average crystallite size of the calcined Eu^{3+}:Y_2O_3 particles. As a result, the particle sizes of Y_2O_3 shown in Figure 4a,b were determined as 26.5 and 29.6 nm, respectively. EDS analysis carried out for Eu^{3+}:Y_2O_3 showed the presence of Eu, Y, and O elements (Figure S1 and Figure S2, Supporting Information).

Morphological Analysis. Figure 5 shows FESEM images of the product as-synthesized in water/1-propanol mixed solvent at 400 °C for 10 min (Figure 5a,b) and after calcination at 1000 °C for 1 h in air (Figure 5c,d). The as-synthesized product consisted of microspheres with 1−2 μm in diameter. The surface of the microsphere was smooth. The product after calcination at 1000 °C retained the microsphere morphology with diameter ranging from 2 to 3 μm as shown in Figure 5c,d. The microsphere after calcinations consisted of the aggregate of small grains of 200−300 nm in diameter.

In contrast, as-synthesized product in water/methanol at 400 °C for 10 min (Figure 6a,b) consisted of well square-built microcubes with 1.5−2.5 μm side length. The surface of the microcube was very smooth (Figure 6b). The product after calcination at 1000 °C (Figure 6c,d) also showed the microcube morphology although the edges were partly collapsed. The side length of the cube was 2−3 μm. The microcubes after calcination consisted of small connected grains. The collapse of the microcube edges might occur due to the rapid gas evolution by dehydration, denitrification, and combustion of organics during calcination (Figure S3, Supporting Information).

As we know, the physicochemical properties of reaction solvent can play an important role for the morphology of the final product.[32] In the present synthesis using the mixed solvents of water/1-propanol and water/methanol under supercritical conditions (400 °C, 40 MPa) resulted in obtaining two different kinds of morphologies, that is, micropheres with water/1-propanol mixed solvent and microcubes with water/methanol mixed solvent, indicating that the use of proper solvents can yield required product with desired morphology.

dx.doi.org/10.1021/ic101496b |*Inorg. Chem.* 2011, 50, 4698–4704

Figure 7a−f shows the FESEM images of the as-synthesized products in mixed solvents of (a−c) water/1-propanol and (d−f) water/methanol at 400 °C for 4, 6, and 8 min. The product in water/1-propanol for 4, 6, and 8 min exhibited agglomerated microspheres of 1−2.5 μm in diameter, although the product after 10 min consisted of well-dispersed microspheres as shown in Figure 6a,b.

In contrast, for the reaction in water/methanol mixed solvent, the morphology of product changed as follows: early stage growth of cube morphology with the side length of 0.5−1 μm for 4 min, interconnected microcubes with the diameter of 0.8−1 μm for 6 min, and then microcubes with the side length of 1−1.2 μm for 8 min, indicating that the particle size increased with time.

Figure 8a−f shows the temperature dependence of morphology of as-synthesized products in the mixed solvents of water/1-propanol (Figure 8a−c) and water/methanol (Figure 8d−f) at 250, 300, and 350 °C for 10 min. The product in water/1-propanol mixed solvent at 250 °C consisted of agglomerated nanoparticles less than 100 nm (Figure 8a). Partly aggregated microspheres of ca. 1.5 μm in diameter were formed at 300 °C (Figure 8b). The product at 350 °C consisted of aggregated microspheres of 1−2 μm in diameter (Figure 8c), which was almost identical to that formed at 400 °C (Figure 5a), but the dispersion of the product at 400 °C seems to be better. In contrast, the product in water/methanol mixed solution at 250 °C consisted of aggregated square-built particles of less than 1 μm in side length, suggesting much larger particle size and higher crystallinity than that in water/1-propanol mixed solvent. The product changed to aggregated cubes with side length less than 1 μm at 300 °C and relatively well formed cubes with side length less than 2.5 μm at 350 °C. These results suggested that the crystallization and grain growth of the product in water/methanol mixed solvent was faster than that in water/1-propanol mixed solvent probably because the dielectric constant of 1-propanol is lower than that of methanol.

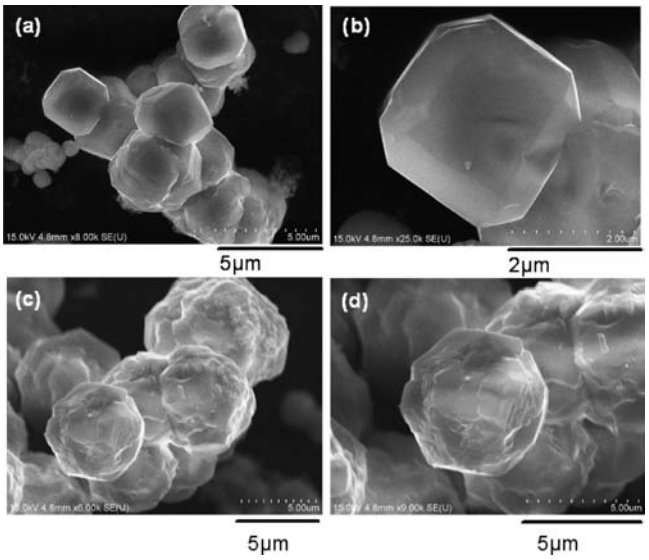

Figure 6. FESEM images of as-synthesized microcubes in water/methanol mixed solvent at 400 °C for 10 min (a, b) and Eu^{3+}:Y_2O_3 microcubes (c, d) prepared by calcination at 1000 °C for 1 h in air.

Growth Mechanism. The growth mechanism of precursors with microsphere and microcube morphology was well understood after the investigation of effect of temperature and reaction time. Based on the experimental results, we found that the solvents 1-propanol and methanol had a key role in morphology control. The microsphere formation takes place via formation of aggregated nanoparticles having sphere morphology. It is accepted that when the crystallinity is low and overall growth rate is slow, sphere shape is favored.[31] The slow growth rate was probably due to the effect of organic solvent since organic solvent possesses low dielectric constant and during the reaction, part of decomposed organic molecules could adsorb on the surface of the particles to depress the grain growth. Under supercritical conditions and high pressure, the formed nanoparticles undergo a dissolution−reprecipitation process to form microspheres. A similar mechanism was observed when ethanol was used as solvent to prepare hollow microspheres.[26] In contrast, when a mixed solution of water/methanol was used as reaction solvents, the crystallization and grain growth of the product proceeded more quickly to form nanocubes, and then aggregation, dissolution, and reprecipitation might occur to form microcubes. It is also probable that the organic molecules formed by the decomposition of methanol selectively adsorbed on specific crystal faces to develop the cube-like morphology.

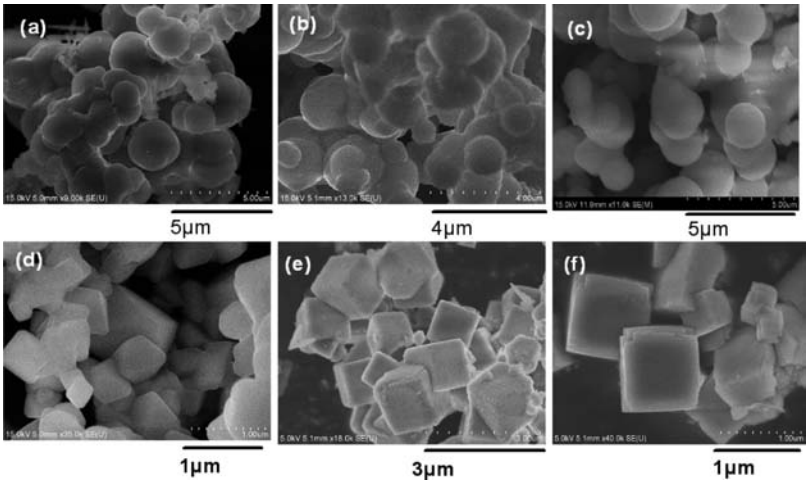

Figure 7. FESEM images of as-synthesized microspheres in water/1-propanol (a, b, and c) and microcubes in water/methanol (d, e, and f) at 400 °C for 4 min (a and d), 6 min (b and e), and 8 min (c and f).

dx.doi.org/10.1021/ic101496b |*Inorg. Chem.* 2011, 50, 4698–4704

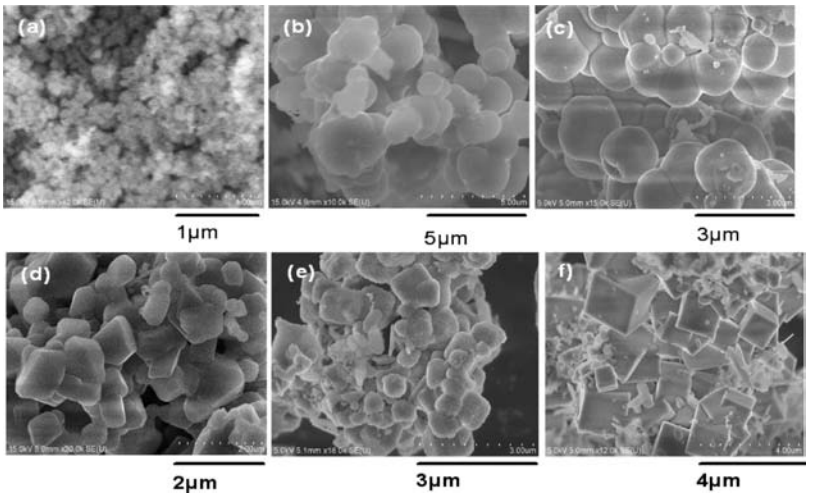

Figure 8. FESEM images of as-synthesized microspheres in water/1-propanol (a, b, and c) and microcubes in water/methanol (d, e, and f) at 250 °C (a and d), 300 °C (b and e), and 350 °C (c and f) for 10 min.

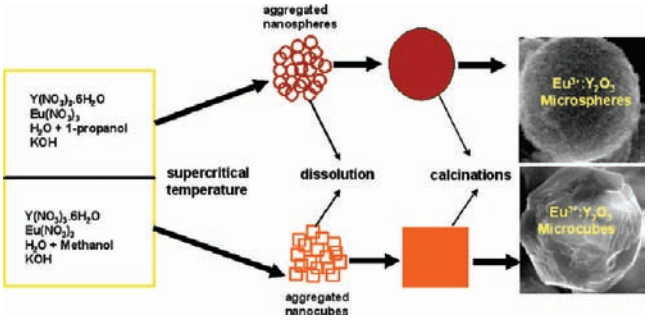

Figure 9. Illustration of formation mechanism of microsphere and microcube precursor particles under supercritical conditions.

Calcination did not lead to the change in the morphology of micrsopheres, since higher activation energy is required for the collapse of these structures.[31] The edges of microcubes were collapsed during calcinations probably due to rapid evolution of gases such as H_2O. CO_2, NO_x, etc. The illustration of formation mechanism of microspheres and microcubes is shown in Figure 9.

Room-Temperature Photoluminescence. Figure 10 shows the room-temperature photoluminescence (PL) emission spectra of Eu^{3+}:Y_2O_3 (5 mol %) microspheres and microcubes after calcinations at 500−1000 °C for 1 h in air. The strongest peak appearing at 610 nm under excitation by 254 nm of UV-light, which was attributed to the forced electric dipole transition ($^5D_0 \rightarrow {}^7F_2$), strongly depends on the Eu^{3+} surrounding due to its electric dipole character. The spectral properties are typical of that reported for Eu^{3+}:Y_2O_3 particles.[33−36] The highly forbidden transition peaks can be seen at 580 nm, and the peaks at 587, 592, and 599 nm are due to the magnetic dipole transition ($^5D_0 \rightarrow {}^7F_1$). This indicates that Eu^{3+} site symmetry has no center of inversion, so the state of opposite parity can be mixed in.[37]

The PL emission intensity of Eu^{3+}:Y_2O_3 microsphere and microcubes increased with increasing calcination temperature, and the highest PL intensity was obtained by calcinations at 1000 °C when compared with the reference sample as shown in Figure 10a. The PL emission intensity can be well compared with that of Eu^{3+}-doped Y_2O_3.[31] It is also notable that for the product

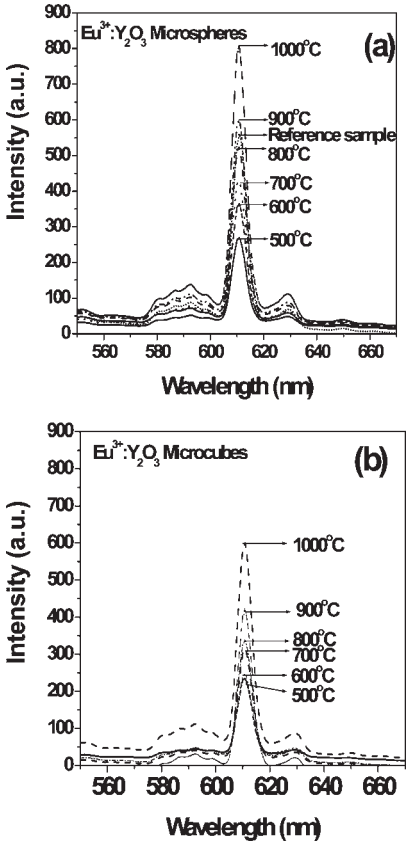

Figure 10. Photoluminscence spectra of Eu^{3+}:Y_2O_3 (a) microspheres and (b) microcubes prepared by calcinations at 500−1000 °C for 1 h in air. Reference sample also included in panel a.

calcined at each temperature the microspheres showed higher PL emission intensity than the microcubes. It agrees with the knowledge that the sphere morphology of the phosphors is good for high brightness and high resolution because of high packing densities and low scattering of light. The phosphor materials synthesized via supercritical conditions have possible potential applications in fluorescent lamps and field emission displays.

dx.doi.org/10.1021/ic101496b |*Inorg. Chem.* 2011, 50, 4698–4704

Table 1. Morphology, Particle Size, Calcination Temperature, and Life Time Measurements

sample name	morphology	calcination temp (°C)	particle size (μm)	lifetime (ms)
Eu^{3+}(5 mol %):Y_2O_3	microsphere	1000	3	1.2
Eu^{3+}(5 mol %):Y_2O_3	microcube	1000	3	1.1
reference sample	irregular	1000	>5	0.9
ref 38	microsphere	800	1−2	1.1

Further, the luminescence lifetime of the $^5D_0 \rightarrow {}^7F_2$ transition at 610 nm was estimated, and the results are shown in Table 1. The lifetime of microspheres, microcubes, and commercial samples are on order of milliseconds. The microspheres and microcubes showed lifetimes of 1.2 and 1.1 ms, respectively, where as the reference sample showed 0.9 ms. The microspheres showed better luminescence lifetime compared with reported microspheres.[38] It should be noted that the luminescence lifetime values reported in some cases are not the same, because they strongly depend on the phosphor size and host lattice, as well as synthesis conditions.[39]

CONCLUSIONS

In summary, we have used supercritical water/1-propanol and water/methanol mixed solvents to successfully synthesize precursor products with microsphere and microcube morphologies, respectively, in a very short reaction time (10 min). Eu^{3+}:Y_2O_3 could be obtained from the as-synthesized product without much change in their morphologies via the calcination process. The as-synthesized product in water/1-propanol mixed solvent consisted of microspheres of 1−1.5 μm in diameter, and the calcined microspheres showed 2−3 μm diameters. In contrast, the as-synthesized product in water/methanol mixed solvent consisted of microcubes of 1.5−2.5 μm, and the calcined product showed 2−3 μm diameters. Both microspheres and microcubes exhibited strong red emission at 610 nm under the excitation wavelength of 254 nm. The emission intensity increased with increasing calcinations temperature from 500 to 1000 °C, and the microspheres showed higher emission intensity and lifetime than microcubes.

ASSOCIATED CONTENT

Supporting Information. EDS and FESEM data. This material is available free of charge via the Internet at http://pubs.acs.org.

AUTHOR INFORMATION

Corresponding Author

*E-mail address: devaraju@tagen.tohoku.ac.jp, devarajumk@rediffmail.com. Tel and Fax: +81-22-217-5597.

Funding Sources

This research was partially supported by the Ministry of Education, Culture, Sports, Science and Technology, Scientific Research of Priority Areas "Panoscopic Assembling and High Ordered Functions for Rare Earth Materials", Special Education and Research Expenses on "Post-Silicon Materials and Devices Research Alliance" and the JSPS Asian Core Program "Interdisciplinary Science of Nanomaterials, JSPS Core University Program (CUP)".

REFERENCES

(1) Xu, A. W.; Cao, Y.; Liu, H. Q. *J. Catal.* **2002**, *207*, 151.
(2) Ronda, C. R. *J. Alloys Compd.* **1995**, *225*, 534.
(3) Jing, X.; Ireland, T; Gibbons, C. *J. Electrochem. Soc.* **1999**, *146* 4654.
(4) Kim, C. H.; Kwon, I. I. E.; Park, C. H.; Hwang, Y. J.; Bae, H. S.; Yu, B. Y.; Pyun, C. H.; Hong, G. Y. *J. Alloys Compd.* **2000**, *311*, 33.
(5) Vecht, A.; Gibbons, C.; Davies, D. *J. Vac. Sci. Technol., B* **1999**, *17*, 750.
(6) Jing, X.; Ireland, T. G.; Gibbons, C.; Barber, D. J.; Silver, J.; Vecht, A.; Fern, G.; Trogwa, P.; Morton, D. *J. Electrochem. Soc.* **1999**, *146*, 4546.
(7) Jiang, Y. D.; Wang, Z. L.; Zhang, F.; Paris, H. G.; Summers, C. J. *J. Mater. Res.* **1998**, *13*, 2950.
(8) Bechtel, H.; Nikol, H. *Proc. Electrochem. Soc.* **1998**, *97*, 256.
(9) Zhou, Y. H.; Lin, J.; Yu, M.; Han, S. M.; Wang, S. B.; Zhang, H. J. *Mater. Res. Bull.* **2003**, *38*, 1289.
(10) Wang, L. S.; Zhou, Y. H.; Quan, Z. W.; Lin *J. Mater. Lett.* **2005**, *59*, 1130.
(11) Wakefield, G.; Holland, E.; Dobson, P. J.; Hutchison, J. L. *Adv. Mater. (Weinheim, Ger.)* **2001**, *13*, 1557.
(12) MacLachlan, M. J.; Manners, I.; Ozin, G. A. *Adv. Mater.* **2000**, *12*, 675.
(13) Hu, J.; Ouyang, M.; Lieber, C. M. *Nature* **1999**, *399*, 48.
(14) Tans, S. J.; Verschueren, A. R. M.; Dekker, C. *Nature* **1998**, *393*, 49.
(15) Zhou, C.; Kong, J.; Yenilmez, E.; Dai, H. *Science* **2000**, *290*, 1552.
(16) Yao, Z.; Postma, H. W. Ch.; Balents, L.; Dekker, C. *Nature* **1999**, *402*, 273.
(17) Antonov, R. D.; Johnson, A. T. *Phys. Rev. Lett.* **1999**, *83*, 3274.
(18) Elias, J.; Tena-Zaera, R.; Levy-Clement, C. *J. Phys. Chem. C* **2008**, *112*, 5736.
(19) Zhang, W. W.; Xu, M.; Zhang, W. P.; Yin, M.; Qi, Z. M.; Xia, S. D.; Claudine, G. *Chem. Phys. Lett.* **2003**, *376*, 318.
(20) Chong, M. K.; Pita, K.; Kam, C. H. *J. Phys. Chem. Solids.* **2005**, *66*, 213.
(21) Jung, K. Y.; Han, K. H. *Electrochem. Solid-State. Lett.* **2005**, *8*, H17.
(22) Sharma, P. K.; Jilavi, M. H.; Nab, R.; Schmidt, H. *J. Mater. Sci. Lett.* **1998**, *17*, 823.
(23) He, Y.; Tian, Y.; Zhu, Y. F. *Chem. Lett.* **2003**, *32*, 862.
(24) Devaraju, M. K.; Yin, S.; Sato, T. *IOP Conf. Series: Mater. Sci. Eng.* **2009**, *1*, No. 01201110.1088/1757-8981/1/1/012011.
(25) Devaraju, M. K.; Yin, S.; Sato, T. *Mater. Sci. Eng. C* **2009**, *29*, 1849–1854.
(26) Devaraju, M. K.; Yin, S.; Sato, T. *Cryst. Growth. Des.* **2009**, *9* (6), 2944–2949.
(27) Rangappa, D.; Naka, T.; Konda, A.; Ishii, M.; Kobayashi, T.; Adschiri, T. *J. Am. Chem. Soc.* **2007**, *126*, 11066.
(28) Rangappa, D.; Ohara, S.; Naka, A.; Konda, T.; Ishii, M.; Adschiri, T. *J. Mater. Chem. Soc.* **2007**, *17*, 4426.
(29) Qun, T.; Zhaoping, L.; Shu., L.; Shuyuan, Z.; Xianming, L.; Yitai, Q. *J. Cryst. Growth.* **2003**, *259*, 208–214.
(30) Ivan, M.; David, C. A.S.; Peter, J. D.; Perry, A. H. *Org. Proc. Res. Dev.* **2000**, *4*, 357–361.
(31) Jun, Y.; Zewei, Q.; Deyan, K; Xiaoming, L; Jun, L. *Cryst. Growth. Des.* **2007**, *7* (4), 731.
(32) Demazeau, G. *J. Mater. Sci.* **2008**, *43*, 2104–2114.
(33) Pao, R. P. *J. Electrochem. Soc.* **1996**, *143*, 189.
(34) Wang, H.; Lin, C. K.; Liu, X. M.; Lin, J. *Appl. Phys. Lett.* **2005**, *87*, No. 181907.
(35) Pang, M. L.; Lin, J.; Cheng, Z. Y. *Mater. Sci. Eng., B* **2003**, *100*, 124.

(36) Igarashi, T.; Ihara, M.; akusunoki, T.; Ohno, K.; Isobe, T.; Senna, M. *Appl. Phys. Lett.* **2000**, *76*, 1549.
(37) Rosa, I. L; Marques, A. P.; Tanaka, M. T.; Melo, D. M.; Leite, E. R.; Longo, E.; Varela, J. A. *J. Fluoresc.* **2008**, *18*, 239–245.
(38) Antic, Ž; Krsmanovic, R; Đor.evic, V; Dramicanin, T; Dramicanin, M. D. *Acta Phys. Pol., A* **2009**, *116*, 622–624.
(39) Phan, L. T.; Phan, H. M.; Vu, Nguyen; Anh, K. T.; Yu, C. S. *Phys. Status Solidi A* **2004**, *9*, 2170–2174.